ROYAL SOCIETY OF CHEMISTRY

www.rsc.org/analyst

Analysis of ATP and AMP binding to the DNA aptamer and its imidazole-tethered derivatives

by surface plasmon resonance†

Jing Zhao,[a] Satoshi Katsube,[b] Junpei Yamamoto,[b] Kazuhiko Yamasaki,[a] Makoto Miyagishi[a]

and Shigenori Iwai*[b]

[a]Biomedical Research Institute, National Institute of Advanced Industrial Science and

Technology, 1-1-1 Higashi, Tsukuba, Ibaraki 305-8566, Japan

[b]Division of Chemistry, Graduate School of Engineering Science, Osaka University, 1-3

Machikaneyama, Toyonaka, Osaka 560-8531, Japan. E-mail: iwai@chem.es.osaka-u.ac.jp;

Tel: +81-6-6850-6250; Fax: +81-6-6850-6240

†Electronic supplementary information (ESI) available: Experimental procedures,

sensorgrams, graphic presentation of the results, and model structures.

Abstract

Imidazole was tethered to the C5 position of thymine in the ATP-binding DNA aptamer with two types of linkers, and the affinities of each aptamer for ATP and AMP were determined by surface plasmon resonance measurements. The imidazole-tethered aptamers exhibited higher affinity for ATP, almost independently of the linker structure or the modification site.

Introduction

Aptamers are single-stranded nucleic acids that bind their target molecules, ranging from small compounds to proteins, with high affinity and specificity.[1,2] They are obtained by a procedure referred to as systematic evolution of ligands by exponential enrichment (SELEX),[3–5] and have been used in various fields, including clinical[6–9] and food safety[10–13] applications. In order to stabilize the aptamers against cellular nucleases, especially in clinical studies, chemical modifications of the sugar moieties and the phosphodiester linkages have been reported.[14,15] On the other hand, Gold *et al.* modified the base moieties in the aptamers to improve their affinities for each target.[16] They used 2'-deoxyuridine 5'-triphosphate bearing hydrophobic substituents at the C5 position for SELEX, in place of thymidine 5'-triphosphate, and designated the obtained aptamers as SOMAmers (Slow Off-rate Modified Aptamers).[16,17] The SOMAmers have been utilized in biomedical studies,[18,19] and the crystal structures of the SOMAmer–protein complexes revealed the hydrophobic interactions and

2

their importance in protein binding.[20,21] In this study, we evaluated imidazole, which was not

used for the SOMAmers, as the C5 substituent, to determine whether this modification would

increase the affinity of an aptamer for its target by hydrogen bond formation or electrostatic

interactions.

When the target is a protein, the aptamer–target interactions might be sterically

hindered by the substituent. Therefore, a DNA aptamer that binds ATP[22] was chosen to test

the possibility of affinity improvement by imidazole tethering. An NMR study of the AMP–

aptamer complex reported a duplex-like structure with two bound AMP molecules, as shown

in Fig. 1A.[23] The adenine base in AMP formed a mismatch pair with guanine in the aptamer,

which was flanked by sheared G·A and reversed Hoogsteen G·G mismatch pairs, and the 5'-

phosphate was located on the far side from the aptamer. In accordance with these aptamer–

target interactions, this aptamer also bound adenosine that lacked the 5'-phosphate.[22] The

aptamer contained four thymine bases, except for the 3'-end residue, and we decided to attach

the imidazole ring to each of these bases (positions a to d in Fig. 1A). In the case of aptamers

containing a G-quadruplex, chemical modifications at the base[24,25] and sugar[26,27] moieties to

improve the binding affinities were investigated, using the existing sequences. However, no

such study has been reported for the duplex-type aptamers.

Materials and methods

Oligonucleotide synthesis

The modified aptamers used in this study were synthesized as described in ESI.

SPR measurements

SPR assays were performed with a BIACORE X (GE Healthcare) apparatus. The 5'-biotinylated oligonucleotides (Table 1) were immobilized on SA sensor chips (GE Healthcare), by injecting 100 nM DNA solutions in phosphate-buffered saline containing 0.005% Tween-20 (PBS-T) into one of the two flow cells (flow cell 2) at a flow rate of 5 µl/min (about 1,600 response units (RUs)), and the other (flow cell 1) was used as a control. Because the sensitivity in the SPR experiments is proportional to the molecular weight of the analyte, the level of the oligonucleotide immobilization was set as high as possible so that binding of relatively small molecules could be detected. Solutions containing different concentrations of ATP and AMP, as described in the legends to Figs. S3, S4, S5, and S8, in PBS-T buffer containing 300 mM NaCl (at a final concentration) and 10 mM $MgCl_2$ were injected into the two flow cells of the sensor chip, at a rate of 20 µl/min for 300 s. After a successive injection of the above PBS-T buffer containing the salts for 300 s, the surface of the sensor chip was washed by injection of 1 M NaCl or 50 mM NaOH for 60 s, when

removal of the analyte was necessary. The sensorgrams shown in Figs. 2, S3–S5, and S8 were

obtained by subtracting the responses in flow cell 1 during the injection of the ATP/AMP

solutions from those in flow cell 2. The average RU values in the sensorgrams at varying

ATP/AMP concentrations were fitted with a 1:1 binding model, using the Origin 9.1 software

to determine the K_d values. The best-fit curves are shown in Figs. 2, S6, and S8, and the K_d

values are listed in Table 1. The stoichiometry was calculated from the RU values and the

molecular weights of the aptamer and the bound ATP/AMP.

Results and discussion

Since the existing aptamer sequence was used, the imidazole-tethered nucleoside was

incorporated by the chemical synthesis of oligonucleotides in this study. To investigate the

effects of the linker structure, two types of phosphoramidite building blocks of 5-substituted

2'-deoxyuridine were prepared. One was a derivative of 5-[(*E*)-3-amino-1-propenyl]-2'-

deoxyuridine (**1** in Fig. 1B), which was originally synthesized to study an RNA-cleaving

DNA enzyme.[28] The other was based on 5-(3-amino-1-propynyl)-2'-deoxyuridine (**2**). As

shown in Fig. S1, the building block (**5**) for the incorporation of **2** was synthesized by the

reaction of the 5'-*O*-(4,4'-dimethoxytrityl)-protected, amino-tethered nucleoside (**3**)[29] with

the *N*-hydroxysuccinimide ester of 2-[1-(2,4-dinitrophenyl)-1*H*-imidazol-4-yl]acetic acid,[30]

5

followed by phosphitylation of the 3'-OH. The oligonucleotides listed in Table 1 were

synthesized using these building blocks, purified by HPLC, and analyzed by electrospray

ionization time-of-flight (ESI-TOF) or matrix-assisted laser desorption/ionization time-of-

flight (MALDI-TOF) mass spectrometry (Table S1). For the analysis by surface plasmon

resonance (SPR) measurements, biotin was attached to the 5' end of each oligonucleotide on

the DNA synthesizer.

To our knowledge, no report has described direct SPR measurements for the analysis

of ATP binding to aptamers, due to the low molecular weight of ATP, although several indirect

methods were developed.[31–34] In this study, the binding of ATP and AMP to the DNA aptamer

(ATP-binding DNA aptamer, ABDA)[22] was successfully analyzed by this method (Fig. 2A).

We optimized the experimental conditions for the SPR measurements, by changing the

concentrations of NaCl and $MgCl_2$ in the buffer, and found that high concentrations of NaCl

(300 mM) and $MgCl_2$ (10 mM) were important for the sensitive SPR detection of the

interactions between the aptamer and ATP/AMP. Although the previous NMR study revealed

that two AMP molecules bound to this aptamer,[23] the stoichiometry determined by SPR was

nearly 1:1, regardless of the structure of the terminal phosphate residue (Table 1). In the NMR

structure, the binding sites are two guanine bases, which form two hydrogen bonds with the

adenine base in each AMP molecule. To determine which binding site was used in the SPR

analysis, we changed each of the two guanine bases to adenine, which lacks the amino

function at the C2 position required for the AMP binding. As shown in Figs. 2B and S3 and

Table 1, both of these mutants (ABDA 9A and 22A) could bind ATP and AMP with a

stoichiometry of about 1:1, although the affinity was reduced. For the double mutant in which

the two binding sites were altered (ABDA 9A22A), no binding was observed (Fig. S3). These

results indicated that either one of the two binding sites is occupied by the target molecule in

the SPR measurement. Thus, the binding of the first and second ATP/AMP molecules is not

simultaneous; instead, it is likely that the affinity for the second ATP/AMP is significantly

weaker than that for the first molecule, presumably because of electrostatic repulsion. In a

previous study using electrospray ionization mass spectrometry, both of the 1:1 and 1:2

complexes were detected for the same aptamer.[35]

Since the ATP and AMP binding to the aptamer were successfully analyzed by the SPR

measurements, the oligonucleotides containing **1** at one of the four thymidine residues in

ABDA (ABDA1-a to d) were tested. An example is shown in Fig. 2C, and all of the results

are presented in Figs. S4 and S6 and Table 1. In general, the incorporation of **1** increased the

affinity of the aptamer for ATP, whereas that for AMP was scarcely affected. The effect of the

imidazole tethering was relatively large at position a, which is closest to the target binding site.

The binding of ATP and AMP to the oligonucleotides containing **2** (ABDA2-a to d) was

investigated next, and similar results were obtained, although the effect was larger at positions

b and c in this case (Figs. 2D, S5, and S6 and Table 1).

The imidazole attached to the C5 position of pyrimidine reportedly increases the

duplex stability by forming a hydrogen bond with the neighboring guanine,[36] but the present

results showing that only the affinity for ATP was increased cannot be explained by this

mechanism. If the thermal stability of the duplex is related to the binding of the target

molecule, then the affinity for AMP should also be increased because the 5'-phosphate is not

recognized by this aptamer.[22,23] We tried to model the imidazole–linker side chains on the

ATP-bound aptamer, using the NMR structure.[23] As shown in Fig. S7, the imidazole ring was

able to interact with the internucleotide linkage near the target binding site in the aptamer, but

it could not reach the 5'-phosphate of ATP in any of them, although the linker in **1** was more

flexible than that in **2**. These results suggested that partial neutralization of the aptamer

backbone by the electrostatic interaction with the positively-charged imidazolium moiety

stabilizes the complex formation when the target molecule contains many negative charges, as

in ATP. The observation that the location of the imidazole moiety only slightly affected the

affinity increase supports this hypothesis. If this mechanism is correct, another basic

functional group should show the same effect on the ATP and AMP binding. To test this

possibility, an amino-tethered nucleoside (Fig. S8A) was incorporated into ABDA, using a

commercially-available building block for the oligonucleotide synthesis. As expected, similar

results were obtained for these aptamers (Fig. S8 and Table 1).

Conclusions

In this study, we showed that the tethering of an imidazole ring or an amino group to the DNA

aptamer could increase its affinity for ATP in a position-independent manner. This is a novel

approach to improve the aptamer affinity, and it may be applicable to other aptamers. The

mechanism by which these functional groups produce this effect will be elucidated by

ongoing studies.

Acknowledgements

The authors thank Tomoko Yamasaki of AIST for her helpful advice on the SPR

measurements.

References

1   F. Radom, P. M. Jurek, M. P. Mazurek, J. Otlewski and F. Jelen, *Biotechnol. Adv.*, 2013,

31, 1260–1274.

2   J. Banerjee and M. Nilsen-Hamilton, *J. Mol. Med.*, 2013, **91**, 1333–1342.

3   D. L. Robertson and G. F. Joyce, *Nature*, 1990, **344**, 467–468.

4   A. D. Ellington and J. W. Szostak, *Nature*, 1990, **346**, 818–822.

5   C. Tuerk and L. Gold, *Science*, 1990, **249**, 505–510.

6   H. Sun, X. Zhu, P. Y. Lu, R. R. Rosato, W. Tan and Y. Zu, *Mol. Ther. Nucleic Acids*, 2014,

    3, e182.

7   J. R. Kanwar, J. S. Shankaranarayanan, S. Gurudevan and R. K. Kanwar, *Drug Discov.*

    Today, 2014, **19**, 1309–1321.

8   W. Zhou, P.-J. J. Huang, J. Ding and J. Liu, *Analyst*, 2014, **139**, 2627–2640.

9   X. Pei, J. Zhang and J. Liu, *Mol. Clin. Oncol.*, 2014, **2**, 341–348.

10 X. Liu and X. Zhang, *Appl. Biochem. Biotechnol.*, 2015, **175**, 603–624.

11 Y. Dong, Y. Xu, W. Yong, X. Chu and D. Wang, *Crit. Rev. Food Sci.*, 2014, **54**, 1548–

    1561.

12 S. Amaya-González, N. de-los-Santos-Álvarez, A. J. Miranda-Ordieres and M. J. Lobo-

    Castañón, *Sensors*, 2013, **13**, 16292–16311.

13 N. Paniel, J. Baudart, A. Hayat and L. Barthelmebs, *Methods*, 2013, **64**, 229–240.

14   H. Y. Kong and J. Byun, *Biomol. Ther.*, 2013, **21**, 423–434.

15   R. E. Wang, H. Wu, Y. Niu and J. Cai, *Curr. Med. Chem.*, 2011, **18**, 4126–4138.

16   L. Gold, D. Ayers, J. Bertino, C. Bock, A. Bock, E. N. Brody, J. Carter, A. B. Dalby, B. E.

     Eaton, T. Fitzwater, D. Flather, A. Forbes, T. Foreman, C. Fowler, B. Gawande, M. Goss,

     M. Gunn, S. Gupta, D. Halladay, J. Heil, J. Heilig, B. Hicke, G. Husar, N. Janjic, T. Jarvis,

     S. Jennings, E. Katilius, T. R. Keeney, N. Kim, T. H. Koch, S. Kraemer, L. Kroiss, N. Le,

     D. Levine, W. Lindsey, B. Lollo, W. Mayfield, M. Mehan, R. Mehler, S. K. Nelson, M.

     Nelson, D. Nieuwlandt, M. Nikrad, U. Ochsner, R. M. Ostroff, M. Otis, T. Parker, S.

     Pietrasiewicz, D. I. Resnicow, J. Rohloff, G. Sanders, S. Sattin, D. Schneider, B. Singer,

     M. Stanton, A. Sterkel, A. Stewart, S. Stratford, J. D. Vaught, M. Vrkljan, J. J. Walker, M.

     Watrobka, S. Waugh, A. Weiss, S. K. Wilcox, A. Wolfson, S. K. Wolk, C. Zhang, and D.

     Zichi, *PLoS ONE*, 2010, **5**, e15004.

17   J. C. Rohloff, A. D. Gelinas, T. C. Jarvis, U. A. Ochsner, D. J. Schneider, L. Gold and N.

     Janjic, *Mol. Ther. Nucleic Acids*, 2014, **3**, e201.

18   S. Kraemer, J. D. Vaught, C. Bock, L. Gold, E. Katilius, T. R. Keeney, N. Kim, N. A.

     Saccomano, S. K. Wilcox, D. Zichi and G. M. Sanders, *PLoS ONE*, 2011, **6**, e26332.

19   S. Gupta, M. Hirota, S. M. Waugh, I. Murakami, T. Suzuki, M. Muraguchi, M. Shibamori,

Y. Ishikawa, T. C. Jarvis, J. D. Carter, C. Zhang, B. Gawande, M. Vrkljan, N. Janjic and D. J. Schneider, *J. Biol. Chem.*, 2014, **289**, 8706–8719.

20 D. R. Davies, A. D. Gelinas, C. Zhang, J. C. Rohloff, J. D. Carter, D. O'Connell, S. M. Waugh, S. K. Wolk, W. S. Mayfield, A. B. Burgin, T. E. Edwards, L. J. Stewart, L. Gold, N. Janjic and T. C. Jarvis, *Proc. Natl. Acad. Sci. USA*, 2012, **109**, 19971–19976.

21 A. D. Gelinas, D. R. Davies, T. E. Edwards, J. C. Rohloff, J. D. Carter, C. Zhang, S. Gupta, Y. Ishikawa, M. Hirota, Y. Nakaishi, T. C. Jarvis and N. Janjic, *J. Biol. Chem.*, 2014, **289**, 8720–8734.

22 D. E. Huizenga and J. W. Szostak, *Biochemistry*, 1995, **34**, 656–665.

23 C. H. Lin and D. J. Patel, *Chem. Biol.*, 1997, **4**, 817–832.

24 S. Goji and J. Matsui, *J. Nucleic Acids*, 2011, **2011**, 316079.

25 K. Y. Lee, H. Kang, S. H. Ryu, D. S. Lee, J. H. Lee and S. Kim, *J. Biomed. Biotechnol.*, 2010, **2010**, 168306.

26 A. Pasternak, F. J. Hernandez, L. M. Rasmussen, B. Vester and J. Wengel, *Nucleic Acids Res.*, 2011, **39**, 1155–1164.

27 C. G. Peng and M. J. Damha, *Nucleic Acids Res.*, 2007, **35**, 4977–4988.

28 S. W. Santoro, G. F. Joyce, K. Sakthivel, S. Gramatikova and C. F. Barbas, *J. Am. Chem.*

Soc., 2000, **122**, 2433–2439.

29   A. Brewer, S. Siligardi, C. Neylon and E. Stulz, *Org. Biomol. Chem.*, 2011, **9**, 777–782.

30   G. Wang and D. E. Bergstrom, *Tetrahedron Lett.*, 1993, **34**, 6725–6728.

31   J. Wang and H. S. Zhou, *Anal. Chem.*, 2008, **80**, 7174–7178.

32   J. Wang, A. Munir, Z. Zhu and H. S. Zhou, *Anal. Chem.*, 2010, **82**, 6782–6789.

33   G.-H. Yao, R.-P. Liang, X.-D. Yu, C.-F. Huang, L. Zhang and J.-D. Qiu, *Anal. Chem.*, 2015, **87**, 929–936.

34   G.-H. Yao, R.-P. Liang, C.-F. Huang, L. Zhang and J.-D. Qiu, *Anal. Chim. Acta*, 2015, **871**, 28–34.

35   K. M. Keller, M. M. Breeden, J. Zhang, A. D. Ellington and J. S. Brodbelt, *J. Mass Spectrom.*, 2005, **40**, 1327–1337.

36   D. Buyst, V. Gheerardijn, K. Fehér, B. Van Gasse, J. Van Den Begin, J. C. Martins and A. Madder, *Nucleic Acids Res.*, 2015, **43**, 51–62.

Table 1 Dissociation constants and stoichiometries for ATP and AMP binding

Aptamer	ATP		AMP	
	K_d (µM)	n[a]	K_d (µM)	n[a]
ABDA[b]	55.2 ± 4.2	1.2	45.6 ± 4.0	1.0
ABDA 9A[c]	506 ± 82	1.4	354 ± 86	1.0
ABDA 22A[c]	277 ± 54	0.7	447 ± 157	0.5
ABDA 9A22A[c]	ND[d]	ND[d]	ND[d]	ND[d]
ABDA1-a[e]	11.2 ± 0.4	1.3	26.3 ± 0.5	1.4
ABDA1-b[e]	21.5 ± 1.8	1.2	34.0 ± 1.5	1.3
ABDA1-c[e]	21.4 ± 2.1	1.5	40.7 ± 4.7	1.4
ABDA1-d[e]	21.1 ± 1.5	1.1	47.3 ± 1.9	1.2
ABDA2-a[e]	29.3 ± 2.6	1.2	42.3 ± 4.1	1.3
ABDA2-b[e]	19.6 ± 1.5	1.5	38.6 ± 2.4	1.6
ABDA2-c[e]	19.4 ± 0.6	1.8	34.0 ± 2.4	2.0
ABDA2-d[e]	24.4 ± 2.1	1.3	58.1 ± 1.9	1.4
ABDA amino-a[f]	25.7 ± 0.7	0.8	56.8 ± 9.4	1.0
ABDA amino-c[f]	24.3 ± 0.9	1.1	45.6 ± 4.0	1.3

[a] Stoichiometry. [b] The sequence is shown in Fig. 1A. [c] The guanine bases at positions 9 and 22 were changed to adenine. [d] Not determined. [e] The numbers and the lower-case letters in the aptamer names represent the linker structures and the modification sites shown in Fig. 1, respectively. [f] The amino-tethered nucleoside shown in Fig. S8A was incorporated at positions a and c in Fig. 1A.

Figure legends

Fig. 1 (A) Structure of the ATP-binding DNA aptamer (ABDA). Canonical and unusual base

pairs are indicated by double and single dots, respectively, and italicized As represent the

adenine bases in ATP or AMP. The modified bases were incorporated at the positions

indicated by a, b, c, and d. (B) Structures of the imidazole-tethered nucleosides. Compounds **1**

and **2** were incorporated into the ABDA1 and ABDA2 series, respectively.

Fig. 2 Sensorgrams and graphic presentations of ATP binding to ABDA (A), ABDA 9A (B),
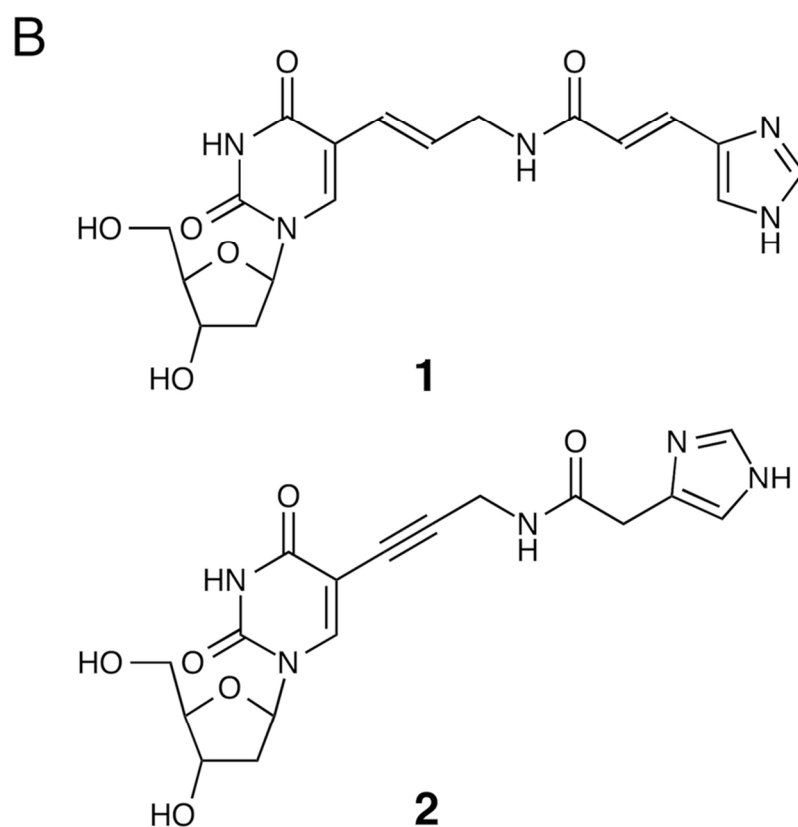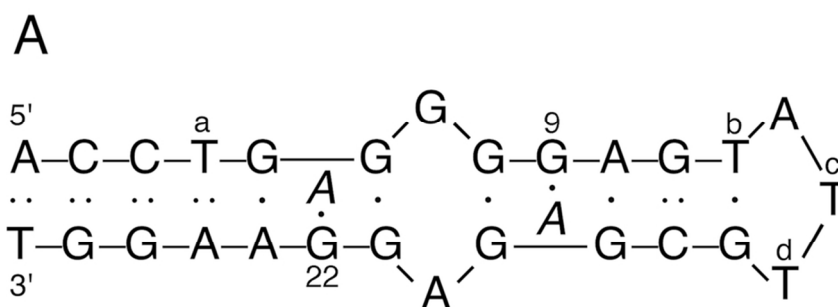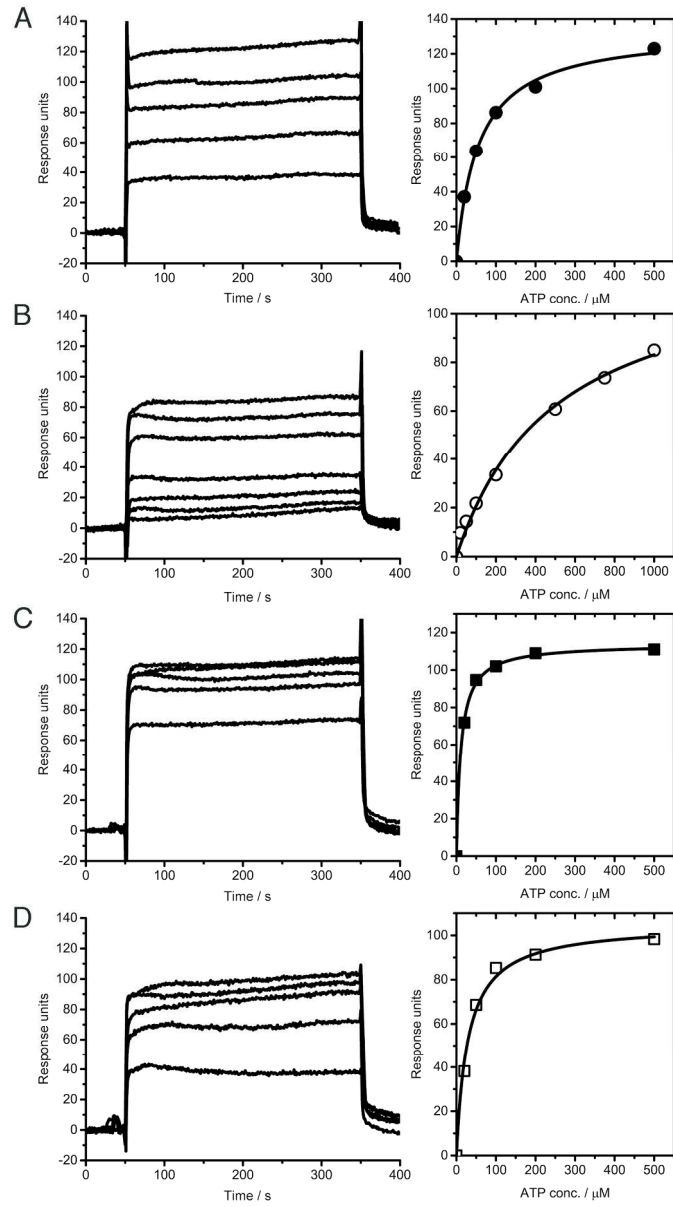
ABDA1-a (C), and ABDA2-a (D).

Fig. 1
82x113mm (300 x 300 DPI)

Fig. 2
149x268mm (300 x 300 DPI)